

LET Spectra of Fragmented 600-MeV/A Iron Beam on Aluminum and Polyethylene

A Preliminary Analysis

*Judy L. Shinn and John W. Wilson
Langley Research Center • Hampton, Virginia*

*E. V. Benton, I. Csige, A. L. Frank, and E. R. Benton
University of San Francisco • San Francisco, California*



Abstract

An iron beam experiment recently conducted at the Lawrence Berkeley Laboratory Bevalac by Benton et al. provides an opportunity for verifying the new Green's function computer code (GRNTRN) and assessing the related nuclear database. The iron beam with 600 MeV/A at extraction traversed a series of beam transport elements, lead foil, and several triggering devices before impacting the target. Of these, only the 2.24 g/cm² lead foil and target are considered in the transport analysis with an assumed (inferred from calibration) beam energy of 557 MeV/A. A thin layer of CR-39 plastic nuclear track detector (PNTD) was placed in front of the target to monitor the incident flux and a stack of four PNTD's placed behind to measure the linear energy transfer (LET) distribution of the transported beam. Test data are analyzed for three separate targets: 2 g/cm² aluminum, 5-cm polyethylene, and 8-cm polyethylene. The two-layer GRNTRN results were mapped into the detector response function for comparison with the measured LET spectra. Reasonable agreement is obtained. Future research and analysis can be improved by using a more accurate isotope set or including other important media which significantly alter the beam. The assumption that the fragmentation cross sections are too small for aluminum is inconclusive because the production of fragments by 2 g/cm² aluminum can be more significantly affected by the fragment contribution originating from the media in front of the target than that currently considered in the analysis.

Introduction

In designing a spacecraft for piloted missions or a commercial high-altitude transport aircraft, consideration must be given to protecting the crews (refs. 1-3) and passengers (refs. 4-10) from exposure to harmful radiation originating in space. This safety consideration requires development of highly efficient shielding computer codes which are practical for integrated system design; a set of shielding computer codes (refs. 11-13) is being developed at the Langley Research Center. Most recently, a new method of using Green's function for the solution of the heavy ion transport equations has resulted in a code that is not only efficient for engineering design application but also suitable for a monoenergetic beam source which could be validated in the laboratory. (See refs. 14-17.) Because of the dearth of experimental measurements of fragmentation cross sections for heavy ion collisions, much uncertainty is associated with the present nuclear cross section database in the computer codes. This uncertainty has had a significant impact on the study of shielding. (See ref. 18.)

An iron beam experiment recently conducted at the Lawrence Berkeley Laboratory Bevalac by E. V. Benton using CR-39 plastic nuclear track

detectors (PNTD's) offers an opportunity for verifying the new Green's function computer code (refs. 16 and 17) and assessing the existing nuclear database. The linear energy transfer (LET) spectra of the attenuated iron beam and ion fragments were obtained by the PNTD's which were placed behind an aluminum or polyethylene degrader. Theoretical results obtained by using the Green's function computer code were compared with the measured LET spectra.

Experiment

Iron beams were accelerated to a 600-MeV/A nominal extraction energy. After extraction, the beam traversed a series of beam transport elements, lead-scattering foils (i.e., beam spreader), and several triggering devices before impacting the target. A series of tests were performed by Benton et al. (University of San Francisco) using various thicknesses of the target materials shown in table I; only the data analysis for the 2 g/cm² aluminum, 5-cm polyethylene, and 8-cm polyethylene targets were completed for this study. Figure 1 shows the experimental arrangement of the lead foil, target, and CR-39 PNTD's considered in the current transport analysis. The remaining media in front of the target and PNTD's which will

affect energy and composition of the beam are being neglected because the 0.198-cm-thick (2.24 g/cm²) lead foil is the major factor in changing the beam. The 557-MeV/A beam energy used for current analysis is inferred from calibration tests by assuming the simple layout in which only the lead foil effect has been considered. The energy spread of the beam has a standard deviation of 0.2 percent.

A thin layer of CR-39 PNTD placed in front of the target monitors the incident beam intensity and a stack of four CR-39 PNTD's behind the target measure the transported LET distribution. Calibration of these detectors with various ion beams of known LET resulted in a detector response function which is approximately Gaussian with an LET-dependent Γ (full-width at half-maximum) as shown in figure 2.

Green's Function Methods

Transport Equations and Conventional Approach

The transport equation for high-energy heavy ions is usually simplified by assuming the straight-ahead approximation and neglecting the target secondary fragments (ref. 19) and is written as

$$\left[\frac{\partial}{\partial x} - \frac{\partial}{\partial E} \tilde{S}_j(E) + \sigma_j \right] \phi_j(x, E) = \sum_k \sigma_{jk} \phi_k(x, E) \quad (1)$$

where $\phi_j(x, E)$ is the ion flux at x with energy E in MeV/A, $\tilde{S}_j(E)$ is the change in E per unit distance, σ_j is the total macroscopic absorption cross section, and σ_{jk} is the macroscopic cross section for the collision of an ion of type k to produce an ion of type j . The solution to equation (1) is subject to the boundary condition

$$\phi_j(0, E) = f_j(E) \quad (2)$$

which for laboratory beams has only one value of j for which $f_j(E) \neq 0$ and that $f_j(E)$ is described by a mean energy E_0 , and an energy spread σ such that

$$f_j(E) = \frac{1}{\sqrt{2\pi}\sigma} \exp\left[\frac{-(E - E_0)^2}{2\sigma^2} \right] \quad (3)$$

The solution to equation (1) is given by superposition of Green's function G_{jk} as

$$\phi_j(x, E) = \sum_k \int G_{jk}(x, E, E') f_k(E') dE' \quad (4)$$

where Green's function is a solution of

$$\left[\frac{\partial}{\partial x} - \frac{\partial}{\partial E} \tilde{S}_j(E) + \sigma_j \right] G_{jm}(x, E, E_0) = \sum_k \sigma_{jk} G_{km}(x, E, E_0) \quad (5)$$

subject to the boundary condition

$$G_{jm}(0, E, E_0) = \delta_{jm} \delta(E - E_0) \quad (6)$$

The above equations can be simplified by transforming the energy into the residual range as

$$r_j = \int_0^E \frac{dE'}{\tilde{S}_j(E')} \quad (7)$$

By defining new field functions as

$$\psi_j(x, r_j) = \tilde{S}_j(E) \phi_j(x, E) \quad (8)$$

$$\mathcal{G}_{jm}(x, r_j, r'_m) = \tilde{S}_j(E) G_{jm}(x, E, E') \quad (9)$$

$$\hat{f}_j(r_j) = \tilde{S}_j(E) f_j(E) \quad (10)$$

equation (5) becomes

$$\left(\frac{\partial}{\partial x} - \frac{\partial}{\partial r_j} + \sigma_j \right) \mathcal{G}_{jm}(x, r_j, r'_m) = \sum_k \frac{\nu_j}{\nu_k} \sigma_{jk} \mathcal{G}_{km}(x, r_k, r'_m) \quad (11)$$

with the boundary condition

$$\mathcal{G}_{jm}(0, r_j, r'_m) = \delta_{jm} \delta(r_j - r'_m) \quad (12)$$

and with the solution of the ion fields given by

$$\psi_j(x, r_j) = \sum_m \int_0^\infty \mathcal{G}_{jm}(x, r_j, r'_m) \hat{f}_m(r'_m) dr'_m \quad (13)$$

Note that ν_j is the range scale factor as $\nu_j r_j = \nu_m r_m$ and is defined as $\nu_j = Z_j^2/A_j$. The solution to equation (11) is written as a perturbation series

$$\mathcal{G}_{jm}(x, r_j, r'_m) = \sum_i \mathcal{G}_{jm}^{(i)}(x, r_j, r'_m) \quad (14)$$

where

$$\mathcal{G}_{jm}^{(0)}(x, r_j, r'_m) = g(j) \delta_{jm} \delta(x + r_j - r'_m) \quad (15)$$

and

$$\mathcal{G}_{jm}^{(1)}(x, r_j, r'_m) \approx \frac{\nu_j \sigma_{jm} g(j, m)}{x(\nu_m - \nu_j)} \quad (16)$$

where $\mathcal{G}_{jm}^{(1)}(x, r_j, r'_m) = 0$ unless

$$\frac{\nu_j}{\nu_m}(r_j + x) \leq r'_m \leq \frac{\nu_j}{\nu_m} r_j + x \quad (17)$$

for $\nu_m > \nu_j$. If $\nu_j > \nu_m$, which can happen in neutron removal, the negative of equation (16) is used and the upper and lower limits of equation (17) are switched. The higher order terms are approximated as

$$\begin{aligned} \mathcal{G}_{jm}^{(i)}(x, r_j, r'_m) \\ \approx \sum_{k_1, k_2, \dots, k_{i-1}} \frac{\nu_j \sigma_{jk_1} \sigma_{k_1 k_2} \dots \sigma_{k_{i-1} m} g(j, k_1, k_2, \dots, k_{i-1}, m)}{x(\nu_m - \nu_j)} \end{aligned} \quad (18)$$

In the above

$$g(j) = \exp(-\sigma_j x) \quad (19)$$

and

$$\begin{aligned} g(j_1, j_2, \dots, j_n, j_{n+1}) \\ = \frac{g(j_1, j_2, \dots, j_{n-1}, j_n) - g(j_1, j_2, \dots, j_{n-1}, j_{n+1})}{\sigma_{j_{n+1}} - \sigma_{j_n}} \end{aligned} \quad (20)$$

Note that the approximation of $\mathcal{G}_{jm}^{(i)}(x, r_j, r'_m)$ by equation (18) is purely dependent on x and for $i > 0$ which is represented as $\mathcal{G}_{jm}^{(i)}(x)$. From above and reference 3, the solution to equation (1) is

$$\begin{aligned} \psi_j(x, r_j) = \exp(-\sigma_j x) \hat{f}_j(r_j + x) \\ + \sum_{m,i} \mathcal{G}_{jm}^{(i)}(x) [\hat{F}_m(r'_{m\ell}) - \hat{F}_m(r'_{mu})] \end{aligned} \quad (21)$$

where r'_{mu} and $r'_{m\ell}$ are given by the upper and lower limits of the inequality (17) and $\hat{F}_m(r'_m)$ refers to the integral spectrum

$$\hat{F}_m(r'_m) = \int_{r'_m}^{\infty} \hat{f}_m(r) dr \quad (22)$$

New Approach With Nonperturbative Method

The higher order terms (third and above) of the perturbative solution derived from equation (21) may be important in the practical applications which require calculations for deep penetration. Because computation of the higher order terms is inefficient particularly for the fragmentation of heavier projectiles, the perturbative approach given above is not suitable for engineering design applications. The following describes a new nonperturbative approach developed recently by Wilson et al. (See ref. 16.)

Reference 17 extends the method to the heavy ion transport in multilayered materials. In this new approach, Green's function is constructed from a convolution product of very thin shield solutions whereby the higher order terms can be neglected.

First, recall that the g function of n arguments was generated by the perturbation solution of the transport equation neglecting ionization energy loss (ref. 20) given by

$$\left(\frac{\partial}{\partial x} + \sigma_j \right) g_{jm}(x) = \sum_k \sigma_{jk} g_{km}(x) \quad (23)$$

subject to the boundary condition

$$g_{jm}(0) = \delta_{jm} \quad (24)$$

for which the solution is

$$g_{jm}(x) = \delta_{jm} g(m) + \sigma_{jm} g(j, m) + \dots \quad (25)$$

It is also true that

$$g_{jm}(x) = \sum_k g_{jk}(x - y) g_{km}(y) \quad (26)$$

for any positive values of x and y . Equation (26) may be used to propagate the function $g_{jm}(x)$ over the solution space from very thin shield solutions. Equation (14) is then rewritten as

$$\begin{aligned} \mathcal{G}_{jm}(x, r_j, r'_m) \approx \exp(-\sigma_j x) \delta_{jm} \delta(x + r_j - r'_m) \\ + \frac{\nu_j [g_{jm}(x) - \exp(-\sigma_j x) \delta_{jm}]}{x(\nu_m - \nu_j)} \end{aligned} \quad (27)$$

and the approximate solution of equation (1) is given by

$$\begin{aligned} \psi_j(x, r_j) = \exp(-\sigma_j x) \hat{f}_j(r_j + x) \\ + \sum_m \frac{\nu_j [g_{jm}(x) - \exp(-\sigma_j x) \delta_{jm}]}{x(\nu_m - \nu_j)} \\ \times [\hat{F}_m(r'_{mu}) - \hat{F}_m(r'_{m\ell})] \end{aligned} \quad (28)$$

Green's Function Methods in a Shielded Medium

The major simplification of the Green's function method results from the fact that the scaled (in transformed variables) spectral distribution of secondary ions to a first approximation depends only on the depth of penetration predicted in equations (16), (18), and (27). The first approach to a multilayered Green's function will rely on this observation and assume its validity for multilayered shields.

Consider a domain labeled as 1 which is shielded by another labeled as 2; the number of ions of type j at depth x in domain 1 due to ions of type m incident on domain 2 of thickness y is

$$g_{12jm}(x, y) = \sum_k g_{1jk}(x) g_{2km}(y) \quad (29)$$

The leading term in equation (29) is the penetrating primaries and all higher order terms are within the bracket of

$$g_{12jm}(x, y) = \exp(-\sigma_{1j}x - \sigma_{2j}y)\delta_{jm} + [g_{12jm}(x, y) - \exp(-\sigma_{1j}x - \sigma_{2j}y)\delta_{jm}] \quad (30)$$

The first term of the scaled Green's function is then

$$\mathcal{G}_{12jm}^{(0)}(x, y, r_j, r'_m) = \exp(-\sigma_{1j}x - \sigma_{2j}y)\delta_{jm}\delta[x + r_j - (r'_m - \rho y)] \quad (31)$$

where ρ is the range scale factor for the two media

$$\rho = \frac{R_{1j}(E)}{R_{2j}(E)} \quad (32)$$

A single value is assumed for ρ corresponding to 600 MeV/A. The secondary contribution is similarly found by noting that equation (17) becomes

$$\frac{\nu_j}{\nu_m}(r_j + x + \rho y) \leq r'_m \leq \frac{\nu_j}{\nu_m} r_j + x + \rho y \quad (33)$$

from which the average spectrum is evaluated. The complete approximation of Green's function is then

$$\mathcal{G}_{12jm}(x, y, r_j, r'_m) \approx \exp(-\sigma_{1j}x - \sigma_{2j}y)\delta_{jm}\delta(x + \rho y + r_j - r'_m) + \frac{\nu_j [g_{12jm}(x, y) - \exp(-\sigma_{1j}x - \sigma_{2j}y)\delta_{jm}]}{(x + \rho y)(\nu_m - \nu_j)} \quad (34)$$

Equation (34) is our first approximation of Green's function in a shielded medium of two layers and is easily modified to multiple layers.

For the first spectral modification, the first collision term has the properties

$$\mathcal{G}_{12jm}^{(1)}(x, y, r_j, r'_m) = \begin{cases} \frac{\nu_j \sigma_{1jm} \exp(-\sigma_{1m}x - \sigma_{2m}y)}{|\nu_m - \nu_j|} & (r'_m = r'_{mu}) \\ \frac{\nu_j \sigma_{2jm} \exp(-\sigma_{1j}x - \sigma_{2j}y)}{|\nu_m - \nu_j|} & (r'_m = r'_{m\ell}) \end{cases} \quad (35)$$

These properties are used to correct the average spectrum to

$$\mathcal{G}_{12jm}^{(1)}(x, y, r_j, r'_m) = \frac{\nu_j g_{12jm}^{(1)}(x, y)}{(x + \rho y)|\nu_m - \nu_j|} + b_{jm}(x, y)(r'_m - \bar{r}_m) \quad (36)$$

where $g_{12jm}^{(1)}(x, y)$ is the first collision term of equation (34) and

$$\bar{r}_m = \frac{r'_{mu} + r'_{m\ell}}{2} \quad (37)$$

is the midpoint of \bar{r}'_m between its limits given by equation (33). The b_{jm} term of equation (36) has the property that

$$\int_{r'_{m\ell}}^{r'_{mu}} b_{jm}(x, y)(r' - \bar{r}'_m) dr' = 0 \quad (38)$$

which ensures that the first term of equation (36) is indeed the average spectrum as required. The spectral slope parameter is

$$b_{jm}(x, y) = \frac{\nu_j \nu_m [\sigma_{1jm} \exp(-\sigma_{1m}x - \sigma_{2m}y) - \sigma_{2jm} \exp(-\sigma_{1j}x - \sigma_{2j}y)]}{(x + \rho y)(\nu_m - \nu_j)|\nu_m - \nu_j|} \quad (39)$$

A similarly simple spectral correction could be made to the higher order terms. The spectral correction given in equation (39) is included in the present Green's function computer code.

Solution for Laboratory Beams

The boundary condition appropriate for laboratory beams is given by equation (3). The cumulative spectrum is given by

$$F_j(E) = \frac{1}{2} \left[1 - \operatorname{erf} \left(\frac{E - E_0}{\sqrt{2}\sigma} \right) \right] \quad (40)$$

The cumulative energy moment needed to evaluate the spectral correction is

$$\bar{E}_j(E) = \frac{1}{2} E_0 \left[1 - \operatorname{erf} \left(\frac{E - E_0}{\sqrt{2}\sigma} \right) \right] + \frac{\sigma}{\sqrt{2}\pi} \exp \left[-\frac{(E - E_0)^2}{2\sigma^2} \right] \quad (41)$$

The average energy on any subinterval (E_1, E_2) is then

$$\bar{E} = \frac{[\bar{E}_j(E_1) - \bar{E}_j(E_2)]}{F_j(E_1) - F_j(E_2)} \quad (42)$$

The beam-generated flux is

$$\begin{aligned} \psi_j(x, y, r_j) = & \exp(-\sigma_1 x - \sigma_2 y) \hat{f}_j(r_j + x + \rho y) \\ & + \sum_{m,i} g_{jm}^{(i)}(x, y) [\hat{F}_m(r'_{mu}) - \hat{F}_m(r'_{m\ell})] \\ & + \sum_m b_{jm}^{(1)}(x, y) [r'_m(\bar{E}) - r'_m] [\hat{F}_m(r'_{mu}) - \hat{F}_m(r'_{m\ell})] \end{aligned} \quad (43)$$

where \bar{E} is evaluated using equation (42) with E_1 and E_2 as the lower and upper limits, respectively, associated with $r'_{m\ell}$ and r'_{mu} .

Nuclear Data Base

The nuclear absorption and fragmentation cross sections needed for the transport calculation are generated by the Langley nuclear fragmentation (NUCFRAG) computer code (ref. 21) by using a reduced set of 80 isotopes as listed in table II. In the past, each charge group was represented by the nearest mass on the stability curve for the associated fragment charge. The most recent versions of the transport computer codes use an isobaric flux representation with the nearest charge on the stability curve; the distance to the nearest isobar was calculated as

$$D = (A_i - A_\ell)^2 + 4(Z_i - Z_\ell)^2 \quad (44)$$

where A_i, Z_i is the fragment and A_ℓ, Z_ℓ is the listed isobar mass and nearest charge to the stability curve used in the calculation. In the following section, a brief description is presented of the nuclear models used in NUCFRAG.

Total Absorption Cross Sections

The nucleon-nucleus absorption cross sections are given by Letaw's formula (ref. 22) that was constructed to fit a consistent set of measurements made by Bobchenko et al. (See ref. 23.) For nucleus-nucleus collisions, an energy-dependent parameterization of a Bradt and Peters (ref. 24) form given by Townsend and Wilson (ref. 25) is used. Recently, a more accurate treatment for light ion-nucleon collisions has been derived in reference 26 in which a normalization factor of 0.95 is added to the parameterized expression of Townsend and Wilson at energies above 80 MeV/A. At energies below 80 MeV/A, a separate expression resulted from the complex quantum mechanical calculation given in reference 26.

Fragmentation Cross Sections

The fragmentation cross section of heavy ions is the least known physics quantity as inputs to the heavy ion transport calculations because of

the dearth of experimental measurements. In the semiempirical nuclear fragmentation model developed for NUCFRAG (ref. 27), the geometric abrasion-ablation model of Bowman, Swiatecki, and Tsang (ref. 28) was modified for the effect of frictional spectator interaction (FSI) by using a semiempirical correction to the abraded prefragment excitation energies. The important effect of the interacting electromagnetic fields (refs. 29 and 30) for heavy ions is also added. For nucleon-nucleus collisions, the fragmentation cross section is generated according to Silberberg and Tsao (refs. 31 and 32) rather than by the abrasion-ablation model. An improvement to fragmentation cross section for the light ions is given in reference 26.

Renormalization

The total absorption and fragmentation cross sections are generated by different models, so a renormalization process is needed to conserve mass and charge. Note that the earlier models of these cross sections failed to conserve mass and charge (ref. 33) and exhibited mass loss of up to 30 percent for $10 \leq Z \leq 22$. The mass loss is displayed in figure 3 in which σ_{abs} is compared with $\sum A_i \sigma_{ip} / A_p$, where A_i is the fragment mass, σ_{ip} is the fragmentation cross section for the projectile p , and A_p is the projectile mass. Because the fragmentation cross section is less certain than the total absorption cross section, the former is renormalized to agree with the latter.

Results

The measured LET distributions behind 2 g/cm² aluminum, 5-cm polyethylene, and 8-cm polyethylene targets are shown in figures 4(a) 4(c), respectively. Also shown are the analytical results obtained by mapping the calculated LET distributions of attenuated iron projectile and projectile fragments into the detector response function where the premapping results were obtained from a two-layer Green's function computer code (GRNTRN) assuming a 2.24 g/cm² lead foil and target combination. Although the shape of the response function is not exactly known, a correction for non-Gaussian contributions is taken as

$$\begin{aligned} R(L, L_0) = & 0.8 \frac{1}{\sqrt{2\pi\sigma_0^2}} \exp\left[-\frac{(L - L_0)^2}{2\sigma_0^2}\right] \\ & + 0.2 \frac{1}{\sqrt{2\pi\sigma_1^2}} \exp\left[-\frac{(L - L_0)^2}{2\sigma_1^2}\right] \end{aligned} \quad (45)$$

where $\sigma_0 = 0.4247\Gamma$ and $\sigma_1 = 2.4\sigma_0$ are fitted to the high-LET side of the measured primary ion peak for a 2 g/cm² aluminum target. (See fig. 4(a).)

Reasonable agreement between the theory and the measured LET distribution was obtained for all the targets; in general, the predicted iron peaks occur at slightly lower LET than the measured peaks, which indicates that the inferred energy of 557 MeV/A may be slightly high. Also, the predicted production of charge 24 and 25 ion groups are much higher than that of the other fragments. This discrepancy may have resulted from the choice of the current isotope set. (See table II.) For the overall fragment flux level, better agreement is noted for the polyethylene targets than for the aluminum target. The assumption that the fragmentation cross sections are too small for aluminum is inconclusive because the low production of fragments by 2 g/cm² aluminum can be more significantly affected by the fragment contribution originating from the media in front of the target than that currently considered in the analysis. For the high-LET side of the primary peak, the least agreement is noted for the 8-cm polyethylene because the non-Gaussian shape corrections were based on the aluminum target and the shape may vary for different LET regions. (Note that the peak for the thicker target appears at a higher LET.)

Concluding Remarks

A preliminary analysis of the measured LET spectra of a fragmented iron beam at 600 MeV/A nominal extraction energy at BEVALAC has been performed for 2 g/cm² aluminum, 5-cm polyethylene, and 8-cm polyethylene targets. Reasonable agreement is obtained between the experimental data and the calculations by using a two-layer (lead foil and target) Green's function computer code. The comparison with experiment could possibly be improved by using a more accurate isotope set or by including in the transport calculation the effect of other important beam-degrading media in front of the target. Future improvements in the code could include energy-dependent nuclear cross sections, the secondary fragment spectra, straggling, and multiple scattering but will have little effect on the results presented in this report.

NASA Langley Research Center
Hampton, VA 23681-0001
February 17, 1994

References

1. Townsend, Lawrence W.; Shinn, Judy L.; and Wilson, John W.: Interplanetary Crew Exposure Estimates for the August 1972 and October 1989 Solar Particle Events. *Radiat. Res.*, vol. 126, 1991, pp. 108–110.
2. Townsend, L. W.; Wilson, J. W.; Shinn, J. L.; and Curtis, S. B.: Human Exposure to Large Solar Particle Events in Space. *Adv. Space Res.*, vol. 12, no. 2–3, 1992, pp. (2)339–(2)348.
3. Shinn, Judy L.; Townsend, Lawrence W.; and Wilson, John W.: Galactic Cosmic Ray Radiation Levels in Spacecraft on Interplanetary Missions. *The World Space Congress—Book of Abstracts*, AIAA, Aug. Sept. 1992, pp. 567–568.
4. Foelsche, Trutz: *Radiation Exposure in Supersonic Transports*. NASA TN D-1383, 1962.
5. Foelsche, Trutz; Mendell, Rosalind B.; Wilson, John W.; and Adams, Richard R.: *Measured and Calculated Neutron Spectra and Dose Equivalent Rates at High Altitudes; Relevance to SST Operations and Space Research*. NASA TN D-7715, 1974.
6. Wilson, John W.; Lambiotte, Jules J., Jr.; Foelsche, Trutz; and Filippas, Tassos A.: *Dose Response Functions in the Atmosphere Due to Incident High-Energy Protons With Application to Solar Proton Events*. NASA TN D-6010, 1970.
7. Foelsche, Trutz: Radiation Safety in High-Altitude Air Traffic. *J. Aircr.*, vol. 14, no. 12, Dec. 1977, pp. 1226–1233.
8. Wilson, J. W.: Solar Radiation Monitoring for High Altitude Aircraft. *Health Phys.*, vol. 41, no. 4, Oct. 1981, pp. 607–617.
9. Fridberg, W.; Faulkner, D. N.; Snyder, L.; Darden, E. B., Jr.; and O'Brien, K.: Galactic Cosmic Radiation Exposure and Associated Health Risk for Air Carrier Crewmembers. *Aviat. Space & Environ. Med.*, vol. 60, no. 11, Nov. 1989, pp. 1104–1108.
10. Wilson, J. W.; and Nealy, J. E.: Radiation Safety in Aircraft Operations. *Proceedings 18th ICAS Congress*, Volume 1, 1992, pp. 541–552.
11. Shinn, Judy L.; Wilson, John W.; Weyland, Mark; and Cucinotta, Francis A.: *Improvements in Computational Accuracy of BRYNTRN (A Baryon Transport Code)*. NASA TP-3093, 1991.
12. Wilson, John W.; Townsend, Lawrence W.; Nealy, John E.; Chun, Sang Y.; Hong, B. S.; Buck, Warren W.; Lamkin, S. L.; Ganapol, Barry D.; Khan, Ferdous; and Cucinotta, Francis A.: *BRYNTRN: A Baryon Transport Model*. NASA TP-2887, 1989.
13. Wilson, John W.; Chun, Sang Y.; Badavi, Forooz F.; Townsend, Lawrence W.; and Lamkin, Stanley L.: *HZETRN: A Heavy Ion-Nucleon Transport Code for Space Radiations*. NASA TP-3146, 1991.
14. Wilson, J. W.; and Badavi, F. F.: New Directions in Heavy Ion Shielding. *Proceedings of the Topical Meeting on New Horizons in Radiation Protection and Shielding*, American Nucl. Soc., Inc., 1992, pp. 205–211.
15. Wilson, John W.; Costen, Robert C.; Shinn, Judy L.; and Badavi, Francis F.: *Green's Function Methods in Heavy Ion Shielding*. NASA TP-3311, 1993.
16. Wilson, John W.; Badavi, Francis F.; Costen, Robert C.; and Shinn, Judy L.: *Nonperturbative Methods for HZE Transport*. NASA TP-3363, 1993.
17. Wilson, John W.; Badavi, Francis F.; Shinn, Judy L.; and Costen, Robert C.: *Approximate Green's Function Methods for HZE Transport in Multilayered Materials*. NASA TM-4519, 1993.
18. Townsend, Lawrence W.; Cucinotta, Francis A.; Shinn, Judy L.; and Wilson, John W.: *Effects of Fragmentation Parameter Variations on Estimates of Galactic Cosmic Ray Exposure—Dose Sensitivity Studies for Aluminum Shields*. NASA TM-4386, 1992.
19. Wilson, John W.: *Analysis of the Theory of High-Energy Ion Transport*. NASA TN D-8381, 1977.
20. Wilson, John W.; Lamkin, Stanley L.; Farhat, Hamidullah; Ganapol, Barry D.; and Townsend, Lawrence W.: *A Hierarchy of Transport Approximations for High Energy Heavy (HZE) Ions*. NASA TM-4118, 1989.
21. Wilson, John W.; Chun, Sang Y.; Badavi, Francis F.; and John, Sarah: *Coulomb Effects in Low-Energy Nuclear Fragmentation*. NASA TP-3352, 1993.
22. Letaw, John R.; Silberberg, R.; and Tsao, C. H.: Proton-Nucleus Total Inelastic Cross Sections: An Empirical Formula for $E > 10$ MeV. *Astrophys. J.*, Suppl. ser., vol. 51, no. 3, Mar. 1983, pp. 271–276.
23. Bobchenko, B. M.; Buklei, A. E.; Viasov, A. V.; Vorob'ev, I. I.; Vorob'ev, L. S.; Goryainov, N. A.; Grishuk, Yu. G.; Gushchin, O. B.; Druzhinin, B. L.; Zhurkin, V. V.; Zavrazhnov, G. N.; Kosov, M. V.; Leksin, G. A.; Stolin, V. L.; Surin, V. P.; Fedorov, V. B.; Fominykh, B. A.; Shvartsman, B. B.; Shevchenko, S. V.; and Shuvalov, S. M.: Measurement of Total Inelastic Cross Sections for Interaction of Protons With Nuclei in the Momentum Range From 5 to 9 GeV/c and for Interaction of π^- Mesons With Nuclei in the Momentum Range From 1.75 to 6.5 GeV/c. *Soviet J. Nucl. Phys.*, vol. 30, no. 6, Dec. 1979, pp. 805–813.
24. Bradt, H. L.; and Peters, B.: The Heavy Nuclei of the Primary Cosmic Radiation. *Phys. Rev.*, second ser., vol. 77, no. 1, Jan. 1, 1950, pp. 54–70.
25. Townsend, L. W.; and Wilson, J. W.: Energy-Dependent Parameterization of Heavy-Ion Absorption Cross Sections. *Radiat. Res.*, vol. 106, 1986, pp. 283–287.

26. Cucinotta, Francis A.; Townsend, Lawrence W.; and Wilson, John W.: *Description of Alpha-Nucleus Interaction Cross Sections for Cosmic Ray Shielding Studies*. NASA TP-3285, 1993.
27. Wilson, John W.; Townsend, Lawrence W.; and Badavi, F. F.: A Semiempirical Nuclear Fragmentation Model. *Nucl. Instrum. & Methods Phys. Res.*, vol. B18, no. 3, Feb. 1987, pp. 225-231.
28. Bowman, J. D.; Swiatecki, W. J.; and Tsang, C. F.: *Abrasion and Ablation of Heavy Ions*. LBL-2908, Univ. of California, July 1973.
29. Norbury, John W.; Cucinotta, F. A.; Townsend, L. W.; and Badavi, F. F.: Parameterized Cross Sections for Coulomb Dissociation in Heavy-Ion Collisions. *Nucl. Instrum. & Methods Phys. Res.*, vol. B31, no. 4, June 1988, pp. 535-537.
30. Norbury, John W.; and Townsend, Lawrence W.: *Electromagnetic Dissociation Effects in Galactic Heavy-Ion Fragmentation*. NASA TP-2527, 1986.
31. Shinn, Judy L.; Wilson, John W.; and Badavi, Francis F.: *Semiempirical Fragmentation Models on Galactic Cosmic Ray Transport Calculations With Hydrogen Target*. NASA TP-3350, 1993.
32. Silberberg, R.; Tsao, C. H.; and Shapiro, M. M.: Semiempirical Cross Sections, and Applications to Nuclear Interactions of Cosmic Rays. *Spallation Nuclear Reactions and Their Applications*, B. S. P. Shen and M. Merker, eds., D. Reidel Publ. Co., 1976, pp. 49-81.
33. Wilson, J. W.: Multiple Scattering of Heavy Ions, Glauber Theory, and Optical Model. *Phys. Lett.*, vol. B52, no. 2, Sept. 1974, pp. 149-152.

Table I. Summary of April 1992 Bevalac Irradiation
600-Mev/A Iron at Extraction

Target	Thickness	Data analysis completed
Al	2 g/cm ²	X
Al	5 g/cm ²	
Al	7 g/cm ²	
Al	10 g/cm ²	
Polyethylene ^a	2 cm	
Polyethylene ^a	5 cm	X
Polyethylene ^a	8 cm	X

^aDensity = 0.92 g/cm².

Table II. Isotopes List

Z	A
0	1
1	1, 2, 3
2	3, 4
3	6, 7
4	8, 9
5	10, 11
6	12, 13
7	14, 15
8	16, 17
9	18, 19
10	20, 21, 22
11	23
12	24, 25, 26
13	27, 28
14	28, 29
15	29, 30, 31
16	31, 32, 33, 34
17	34, 35, 36, 37
18	36, 38, 39, 40
19	37, 39, 40, 41
20	40, 41, 42, 43
21	43, 44, 45, 46
22	44, 45, 46, 47, 48, 49
23	48, 49, 50, 51, 52
24	50, 51, 52, 53
25	53, 54, 55
26	55, 56
27	57
28	58

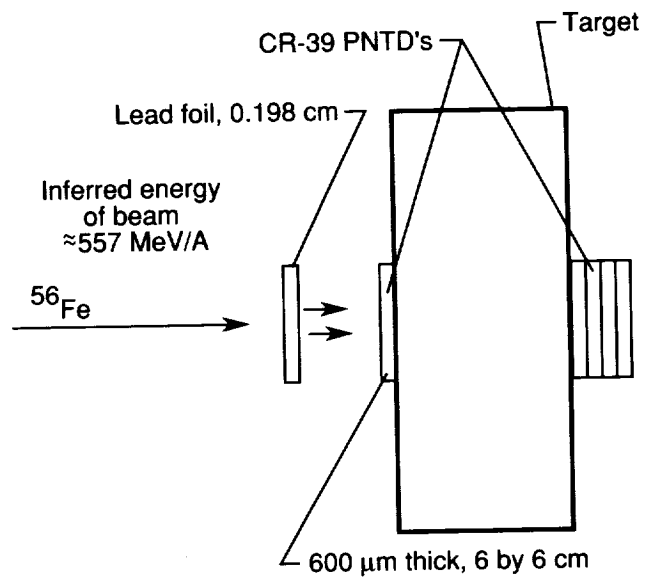


Figure 1. Experimental arrangement.

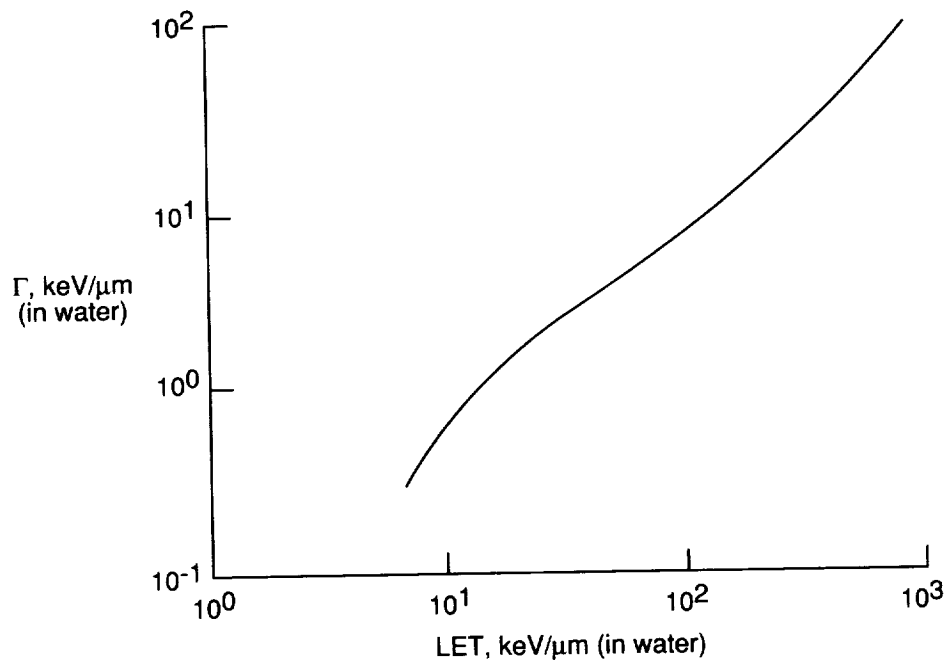


Figure 2. CR-39 detector response function.

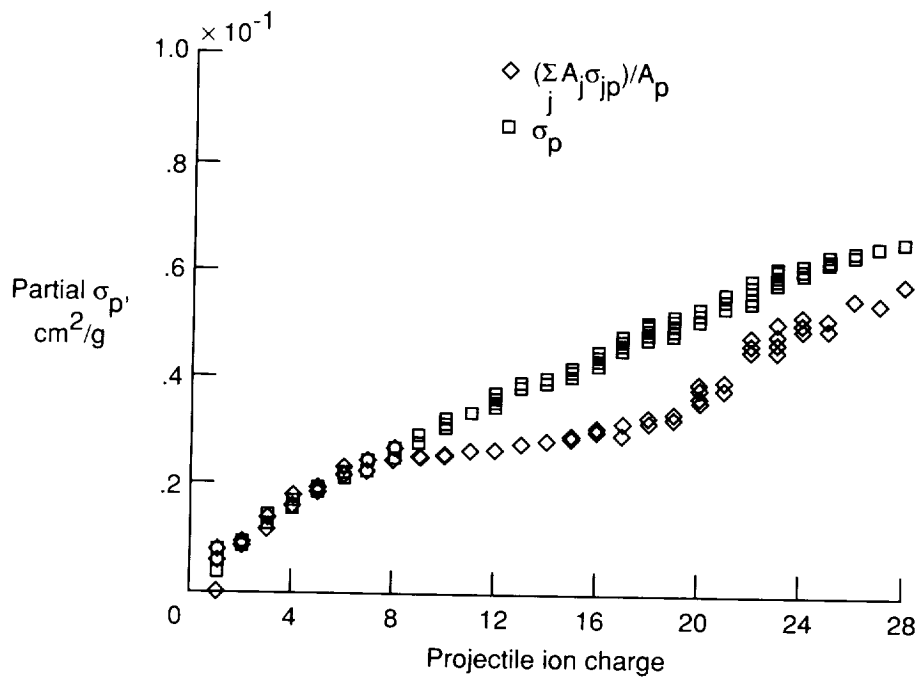
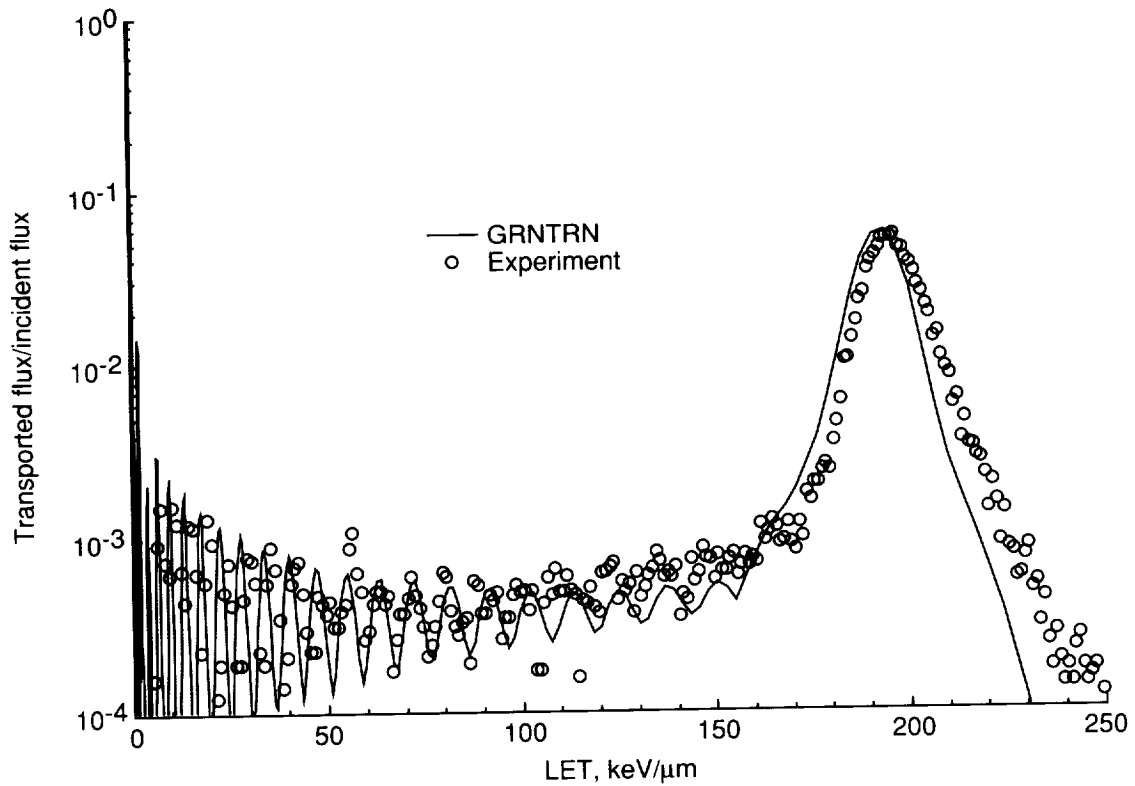
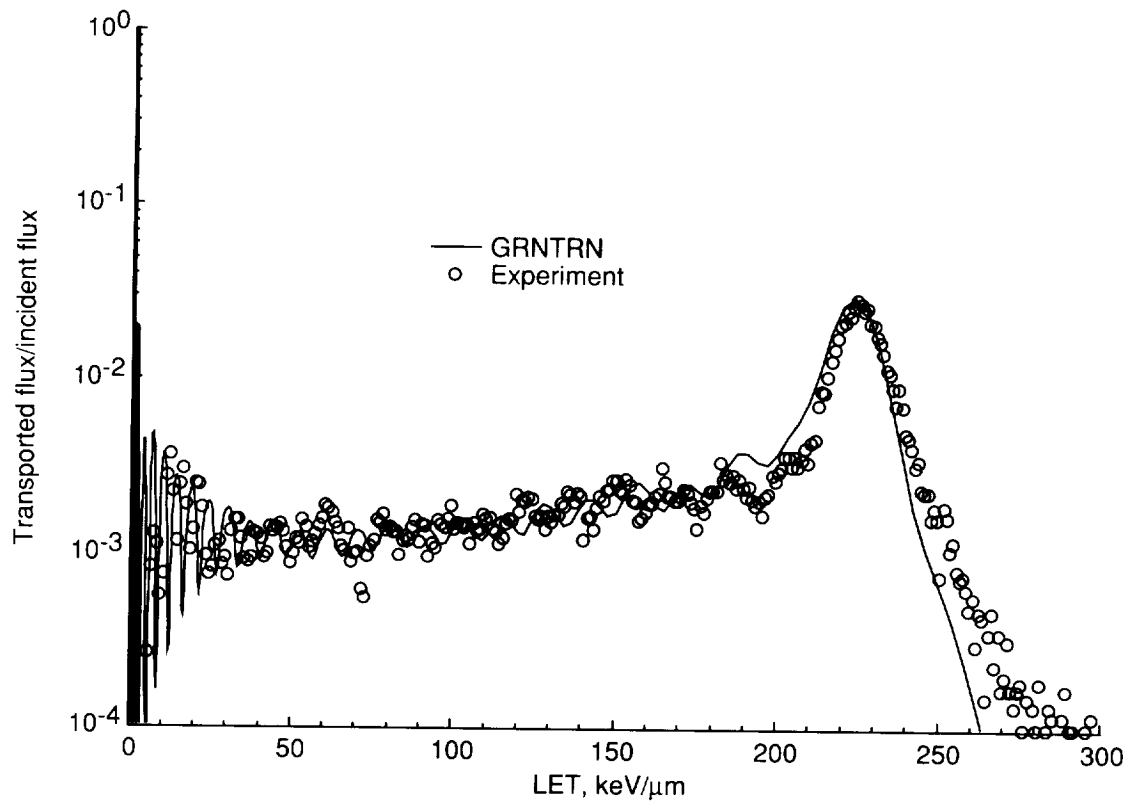


Figure 3. Absorption cross sections in hydrogen component of polyethylene target and mass-average production cross sections for various projectiles at 600 MeV/A.



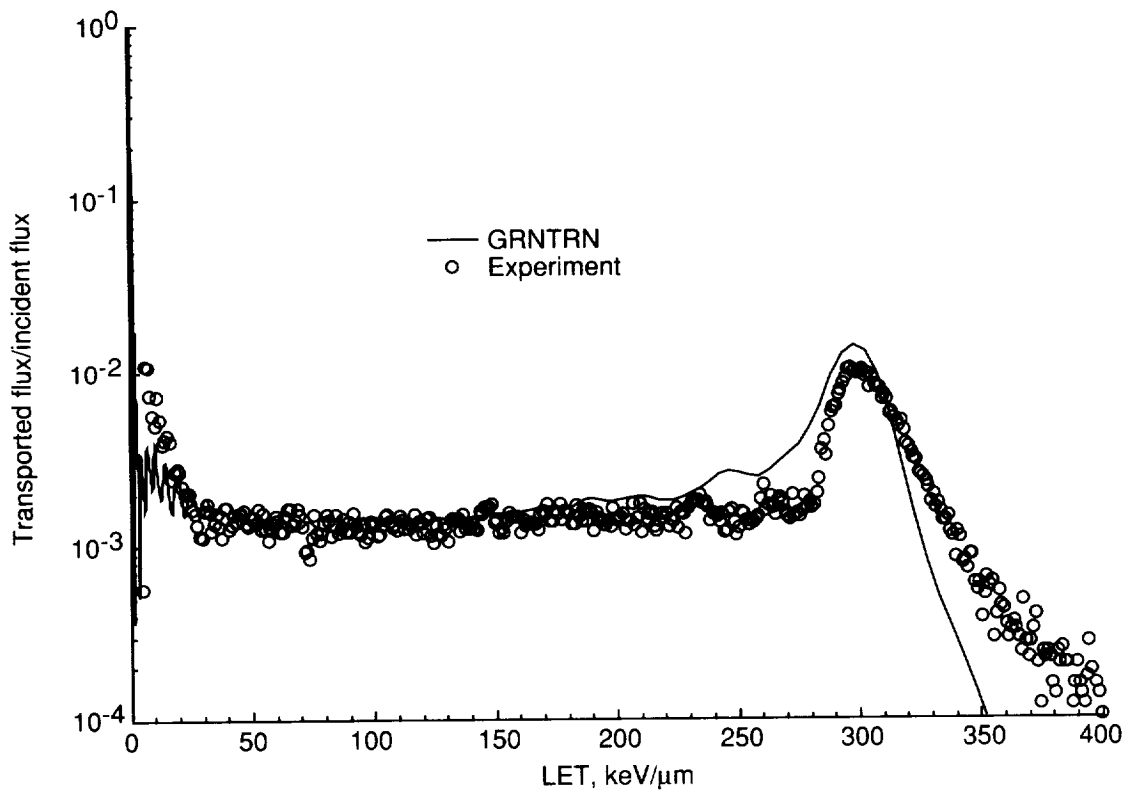
(a) 2 g/cm^2 aluminum target.

Figure 4. Comparison of two-layer (2.24 g/cm^2 lead and target) Green's function calculation (GRNTRN) for 557-MeV/A iron beam and measured LET distribution.



(b) 5-cm polyethylene target.

Figure 4. Continued.



(c) 8-cm polyethylene target.

Figure 4. Concluded.

REPORT DOCUMENTATION PAGE			Form Approved OMB No. 0704-0188	
Public reporting burden for this collection of information is estimated to average 1 hour per response, including the time for reviewing instructions, searching existing data sources, gathering and maintaining the data needed, and completing and reviewing the collection of information. Send comments regarding this burden estimate or any other aspect of this collection of information, including suggestions for reducing this burden, to Washington Headquarters Services, Directorate for Information Operations and Reports, 1215 Jefferson Davis Highway, Suite 1204, Arlington, VA 22202-4302, and to the Office of Management and Budget, Paperwork Reduction Project (0704-0188), Washington, DC 20503				
1. AGENCY USE ONLY (Leave blank)	2. REPORT DATE April 1994	3. REPORT TYPE AND DATES COVERED Technical Paper		
4. TITLE AND SUBTITLE LET Spectra of Fragmented 600-MeV/A Iron Beam on Aluminum and Polyethylene <i>A Preliminary Analysis</i>			5. FUNDING NUMBERS WU 199-45-16-11	
6. AUTHOR(S) Judy L. Shinn, John W. Wilson, E. V. Benton, I. Csige, A. L. Frank, and E. R. Benton				
7. PERFORMING ORGANIZATION NAME(S) AND ADDRESS(ES) NASA Langley Research Center Hampton, VA 23681-0001			8. PERFORMING ORGANIZATION REPORT NUMBER L-17342	
9. SPONSORING/MONITORING AGENCY NAME(S) AND ADDRESS(ES) National Aeronautics and Space Administration Washington, DC 20546-0001			10. SPONSORING/MONITORING AGENCY REPORT NUMBER NASA TP-3436	
11. SUPPLEMENTARY NOTES Shinn and Wilson: Langley Research Center, Hampton, VA; Benton, Csige, Frank, and Benton: University of San Francisco, San Francisco, CA				
12a. DISTRIBUTION/AVAILABILITY STATEMENT Unclassified - Unlimited Subject Category 85 26			12b. DISTRIBUTION CODE	
13. ABSTRACT (Maximum 200 words) An iron beam experiment recently conducted at the Lawrence Berkeley Laboratory Bevalac by Benton et al. provides an opportunity for verifying the new Green's function computer code (GRNTRN) and assessing the related nuclear database. The iron beam with 600 MeV/A at extraction traversed a series of beam transport elements, lead foil, and several triggering devices before impacting the target. Of these, only the 2.24 g/cm ² lead foil and target are considered in the transport analysis with an assumed (inferred from calibration) beam energy of 557 MeV/A. A thin layer of CR-39 plastic nuclear track detector (PNTD) was placed in front of the target to monitor the incident flux and a stack of four PNTD's placed behind to measure the linear energy transfer (LET) distribution of the transported beam. Test data are analyzed for three separate targets: 2 g/cm ² aluminum, 5-cm polyethylene, and 8-cm polyethylene. The two-layer GRNTRN results were mapped into the detector response function for comparison with the measured LET spectra. Reasonable agreement is obtained. Future research and analysis can be improved by using a more accurate isotope set or including other important media which significantly alter the beam. The assumption that the fragmentation cross sections are too small for aluminum is inconclusive because the production of fragments by 2 g/cm ² aluminum can be more significantly affected by the fragment contribution originating from the media in front of the target than that currently considered in the analysis.				
14. SUBJECT TERMS Heavy ion transport; Green's function; Etch track detectors			15. NUMBER OF PAGES 15	
			16. PRICE CODE A02	
17. SECURITY CLASSIFICATION OF REPORT Unclassified	18. SECURITY CLASSIFICATION OF THIS PAGE Unclassified	19. SECURITY CLASSIFICATION OF ABSTRACT	20. LIMITATION OF ABSTRACT	